Supplement of Geosci. Model Dev., 15, 3387–3404, 2022
https://doi.org/10.5194/gmd-15-3387-2022-supplement

Geoscientific Model Development
Open Access
EGU

Supplement of

Precipitation over southern Africa: is there consensus among global climate models (GCMs), regional climate models (RCMs) and observational data?

Maria Chara Karypidou et al.

Correspondence to: Maria Chara Karypidou (karypidou@geo.auth.gr)

Precipitation over southern Africa: Is there consensus among GCMs, RCMs and observational data?

Table S1: Observational datasets used.

Dataset	Resolution	Frequency	Type	Period	Reference
ARC.v2	0.1º	Daily total	Satellite	1983-present	(Novella and Thiaw, 2013)
PERSIANN-CDR	0.25º	Daily total	Satellite	1983-present	(Ashouri et al., 2015)
CMAP	2.5º	Monthly mean	Satellite	1979-present	(Xie and Arkin, 1997)
TAMSAT.v3	0.0375 º	Daily total	Satellite	1983-present	(Tarnavsky et al., 2014; Maidment et al., 2017)
GPCP.v2	2.5º	Monthly mean	Satellite	1979-2015	(Adler et al., 2012)
CRU TS4.01	0.5º	Monthly total	Gauge-Based	1901-2016	(Harris et al., 2014)
GPCC.v7	0.5º	Monthly total	Gauge-Based	1901-2013	(Schneider et al., 2015)
PREC/L	0.5º	Monthly mean	Gauge-Based	1948-2012	(Chen et al., 2002)
UDEL.v4.01	0.5º	Monthly total	Gauge-Based	1900-2014	(Willmott and Matsuura, 1995)
CPC-Unified	0.5º	Daily total	Gauge-Based	1979-present	(Chen et al., 2008)
CHIRPS.v2	0.05º	Daily total	Satellite	1981-present	(Funk et al., 2015)
ERA5	~0.28125 º	Hourly	Reanalysis	1979-present	(C3S, 2017; Hersbach et al., 2020)

Table S2: General circulation models participating in the Coupled Model Intercomparison Project Phase 5 (CMIP5) that were used as forcing fields in the Coordinated Regional Climate Downscaling Experiment (CORDEX) – Africa historical simulations. Data for precipitation were retrieved from the Earth System Grid Federation (https://esgf-data.dkrz.de/projects/esgf-dkrz/). Data for temperature at 850 hPa were retrieved from the Climate Data Store (https://cds.climate.copernicus.eu/#!/home).

GCM	Institute	Ensemble	Latitude Res.	Longitude Res.	References
CanESM2	Canadian Centre for Climate Modelling and Analysis (CCCma)	r1i1p1	2.7906 º	2.8125 º	(CCCma, 2017)
CNRM-CM5	Centre Europeen de Recherche et de Formation Avancee en Calcul Scientifique (CERFACS)	r1i1p1	1.40008 º	1.40625 º	(Voldoire et al., 2013)
CSIRO-Mk3-6-0	Commonwealth Scientific and Industrial Research Organization (CSIRO)	r1i1p1	1.8653 º	1.875 º	(Jeffrey et al., 2013)
EC-EARTH	Sveriges Meteorologiska och Hydrologiska Institut (SMHI),	r1i1p1 r12i1p1	1.1215 º	1.125 º	(Hazeleger et al., 2010)

	Danmarks Meteorologiske Insitut (DMI)				
GFDL-ESM-2M GFDL-ESM-2G	National Oceanic and Atmospheric Administration (NOAA)	r1i1p1	2.0225 ^{o}	2.5 ^{o}	(Dunne et al., 2012)
HadGEM2-ES	Met Office Hadley Centre	r1i1p1	1.25 ^{o}	1.875 ^{o}	(Collins et al., 2011)
IPSL-CM5A-MR IPSL-CM5A-LR	Institut Pierre Simon Laplace (IPSL)	r1i1p1	1.2676 ^{o} 1.894737 ^{o}	2.5 ^{o} 3.75 ^{o}	(Dufresne et al., 2013)
MIROC5	Atmospheric and Ocean Research Institute (AORI)	r1i1p1	1.4008 ^{o}	1.40625 ^{o}	(Watanabe et al., 2010)
MPI-ESM-LR	Max Planck Institute for Meteorology (MPI)	r1i1p1	1.8653 ^{o}	1.875 ^{o}	(Giorgetta et al., 2013)
NorESM1-M	EarthClim	r1i1p1	1.894737 ^{o}	2.5 ^{o}	(Bentsen et al., 2013)

Table S3: General circulation models participating in the Coupled Model Intercomparison Project Phase 6 (CMIP6). Data were retrieved from the Earth System Grid Federation (https://esgf-data.dkrz.de/projects/esgf-dkrz/). The CMIP6 models used were selected in accordance to their predeseccor CMIP5, so that the 2 ensembles (CMIP5 and CMIP6) would be comparable.

GCM	Institute	Ensemble	Latitude Res.	Longitude Res.	References
CanESM5	Canadian Centre for Climate Modelling and Analysis (CCCma)	r1i1p1f1	2.8 ^{o}	2.8 ^{o}	(Swart et al., 2019)
CNRM-CM6-1	Centre Europeen de Recherche et de Formation Avancee en Calcul Scientifique (CERFACS)	r1i1p1f2	1.4^{o}	1.4 ^{o}	(Voldoire et al., 2019)
EC-EARTH3	Sveriges Meteorologiska och Hydrologiska Institut (SMHI), Danmarks Meteorologiske Insitut (DMI)	r1i1p1f1	0.7 ^{o}	0.7 ^{o}	(Massonnet et al., 2020)
GFDL-ESM4	National Oceanic and Atmospheric Administration (NOAA)	r1i1p1f1	1 ^{o}	1.3 ^{o}	(Held et al., 2019)
IPSL-CM6A-LR	Institut Pierre Simon Laplace (IPSL)	r1i1p1f1	1.3 ^{o}	2.5 ^{o}	-

MIROC6	Atmospheric and Ocean Research Institute (AORI)	r1i1p1f1	1.4 ^{o}	1.4 ^{o}	(Tatebe et al., 2019)
MPI-ESM-2-LR	Max Planck Institute for Meteorology (MPI)	r1i1p1f1	1.9 ^{o}	1.9 ^{o}	(Mauritsen et al., 2019)
NorESM2-LM	EarthClim	r1i1p1f1	1.894737 ^{o}	2.5 ^{o}	(Seland et al., 2020)

Table S4: Regional climate model simulations participating in the Coordinated Regional Climate Downscaling Experiment (CORDEX) – Africa ensemble used in the current analysis, with a spatial resolution equal to 0.44^{o} (CORDEX0.44). Data were retrieved from the Earth System Grid Federation (https://esgf-data.dkrz.de/projects/esgf-dkrz/).

RCM	Institute	Forcing	Realization	References
CCLM4-8-17.v1	Climate Limited-area Modelling Community (CLMcom)	CNRM-CM5 EC-EARTH HadGEM2-ES MPI-ESM-LR	r1i1p1 r12i1p1 r1i1p1 r1i1p1	(COSMO, 2020)
RACMO22T.v1	Royal Netherlands Meteorological Institute (KNMI)	EC-EARTH EC-EARTH HadGEM2-ES	r1i1p1 r12i1p1 r1i1p1	(van Meijgaard et al., 2008)
RCA4.v1	Swedish Meteorological and Hydrological Institute (SHMI)	CanESM2 CNRM-CM5 CSIRO-Mk3-6-0 EC-EARTH EC-EARTH IPSL-CM5A-MR HadGEM2-ES MPI-ESM-LR NorESM1-M GFDL-ESM2M MIROC5	r1i1p1 r1i1p1 r1i1p1 r12i1p1 r1i1p1 r1i1p1 r1i1p1 r1i1p1 r1i1p1 r1i1p1 r1i1p1	(Samuelsson et al., 2015)
REMO2009.v1	Max Planck Institut (MPI) and Climate Service Center Germany (CSC)	EC-EARTH MPI-ESM-LR IPSL-CM5A-MR MIROC5 HadGEM2-ES GFDL-ESM2G	r12i1p1 r1i1p1 r12i1p1 r1i1p1 r1i1p1 r1i1p1	(Jacob et al., 2012)
CRCM5.v1	Canadian Centre for Climate Modelling and Analysis (CCCma)	CanESM2 MPI-ESM-LR	r1i1p1 r1i1p1	(Scinocca et al., 2015)

Table S5: Regional climate model simulations participating in the Coordinated Regional Climate Downscaling Experiment (CORDEX) – Africa ensemble used in the current analysis, with a spatial resolution equal to 0.22° (CORDEX0.22). Data were retrieved from the Earth System Grid Federation (https://esgf-data.dkrz.de/projects/esgf-dkrz/).

RCM	Forcing	Realization	Variables available
CanRCM4	CanESM2	r1i1p1	Pr
CCLM5-0-15 REMO2015 RegCM4-7	HadGEM2-ES	r1i1p1 r1i1p1 r1i1p1	Pr, hus850, ua850, va850, ta850
CCLM5-0-15 REMO2015 RegCM4-7	MPI-ESM-LR	r1i1p1 r1i1p1 r1i1p1	Pr, hus850, ua850, va850, ta850
CCLM5-0-15 REMO2015 RegCM4-7	NorESM1-M	r1i1p1 r1i1p1 r1i1p1	Pr, hus850, ua850, va850, ta850

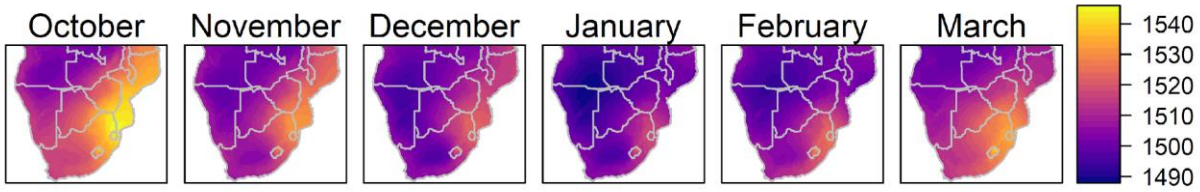

Figure S1: Mean monthly geopotential height at 850 hPa in ERA5 for the period 1986-2005.

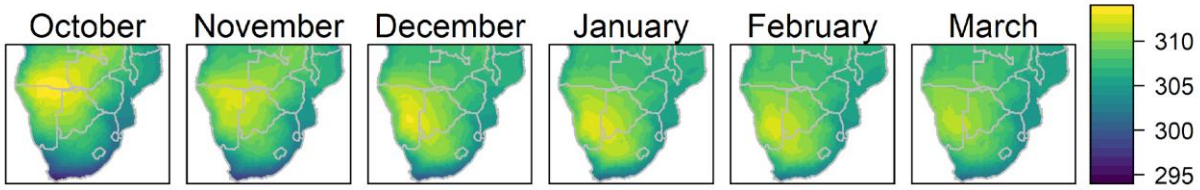

Figure S2: Mean monthly potential temperature at 850 hPa in ERA5 for the period 1986-2005.

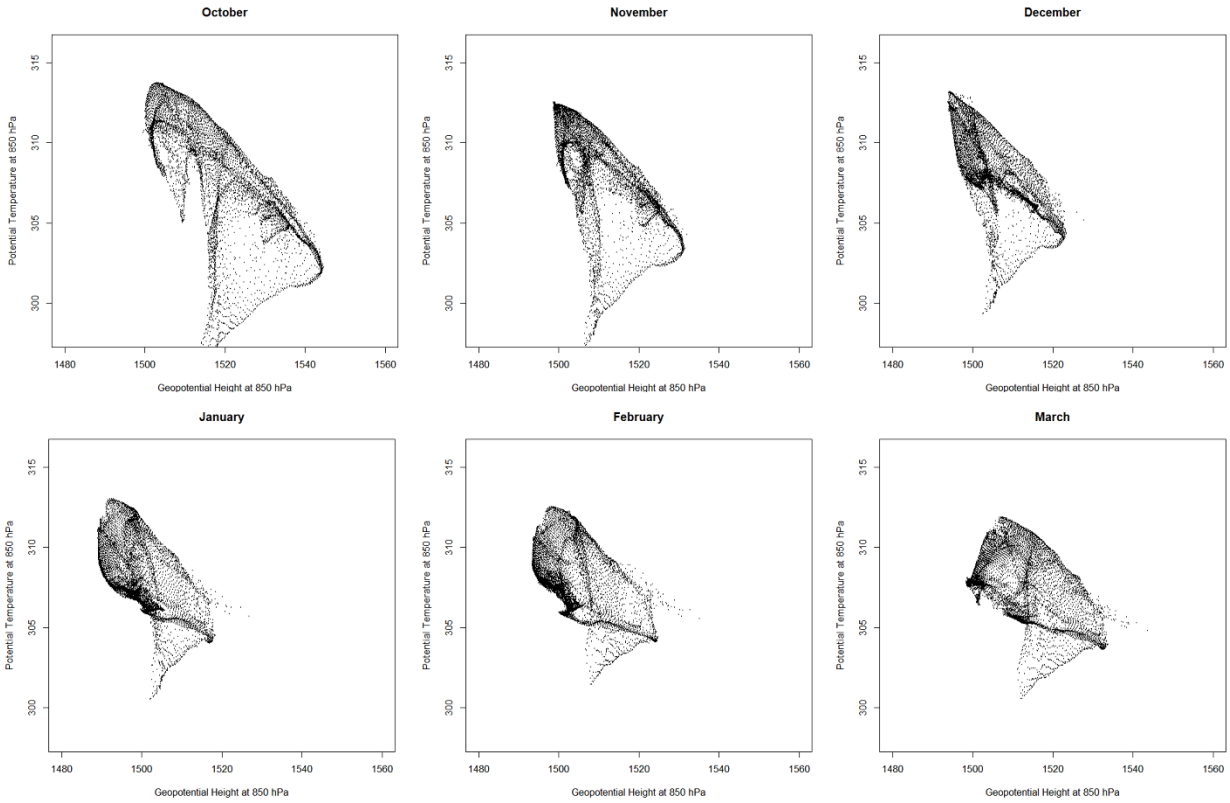

Figure S3: Geopotential height at 850 hPa (x-axis) plotted against potential temperature at 850 hPa (y-axis). Values refer to climatological monthly means for the period 1986-2005. Each dot in the scatterplot represents a pixel of the ERA5 dataset over the whole southern Africa region 10 ºE to 42 ºE and from 10 ºS to 35 ºS.

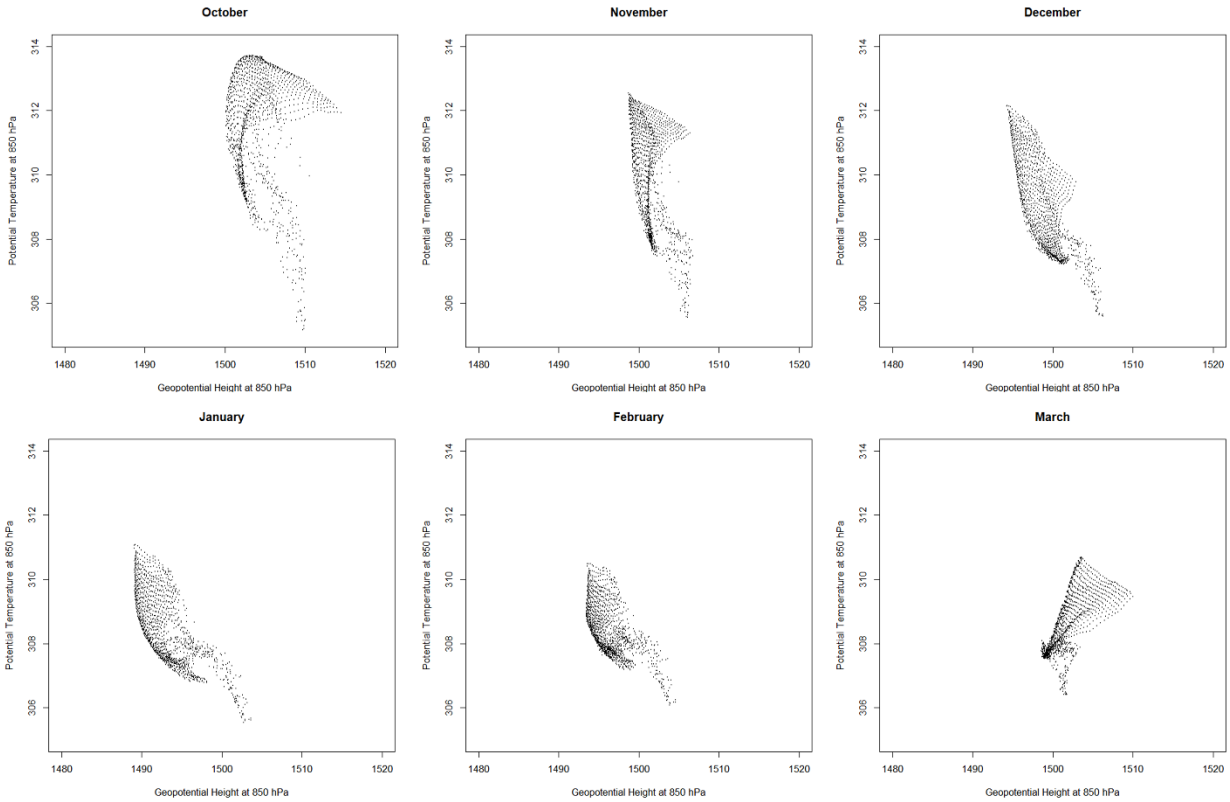

Figure S4: Geopotential height at 850 hPa (x-axis) plotted against potential temperature at 850 hPa (y-axis). Values refer to climatological monthly means for the period 1986-2005. Each dot in the scatterplot represents a pixel of the ERA5 dataset over the greater Angola region from 14 ºE to 25 ºE and from 11 ºS to 19 ºS.

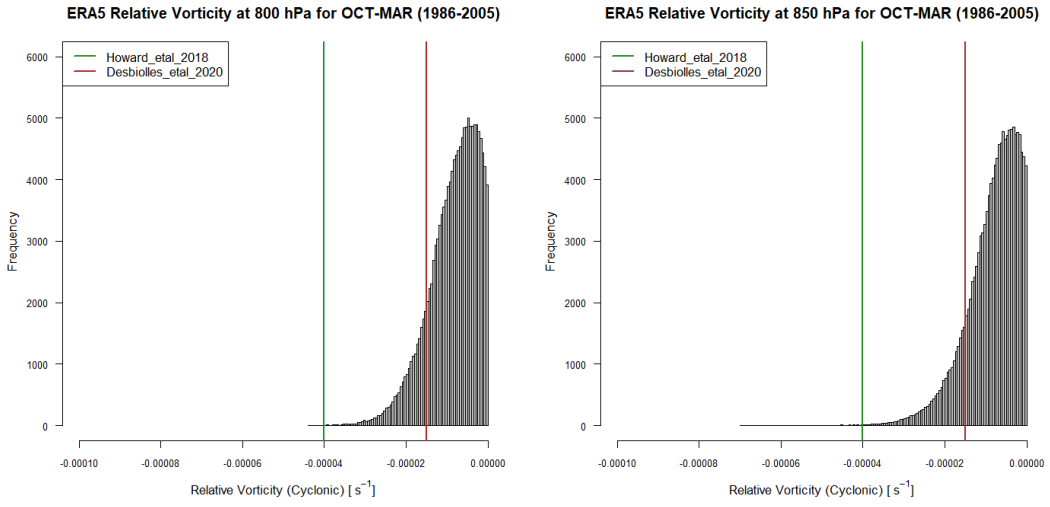

Figure S5: Histogram of relative vorticity for months Oct-Mar during 1986-2005 in ERA5 using u and v values at 800 hPa (left) and at 850 hPa (right). Pixels used are enclosed by the region from 14 ºE to 25 ºE and from 11 ºS to 19 ºS. For both histograms mean monthly u and v values are used.

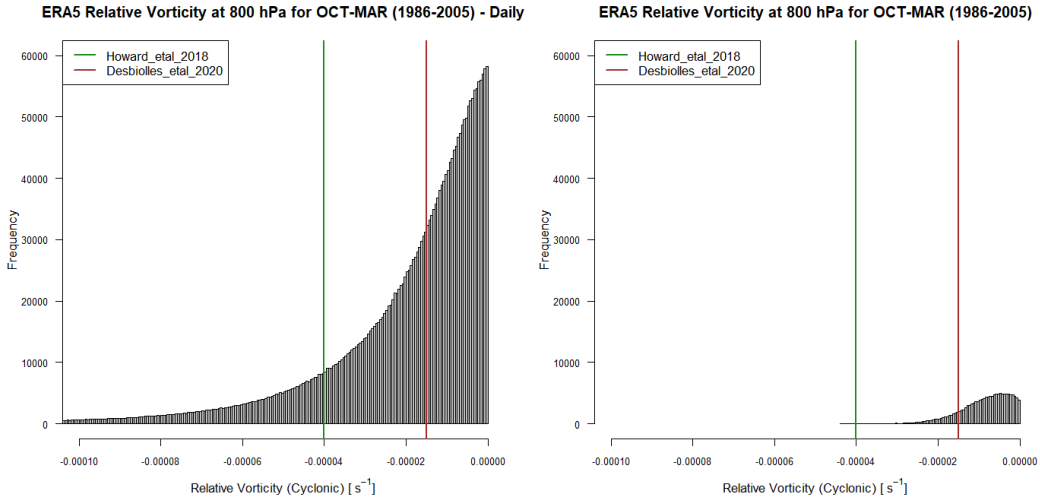

Figure S6: Histogram of relative vorticity for months Oct-Mar during 1986-2005 in ERA5 using daily u and v values (left) and using monthly u and v values (right). Pixels used are enclosed by the region from 14 ^{o}E to 25 ^{o}E and from 11 ^{o}S to 19 ^{o}S.

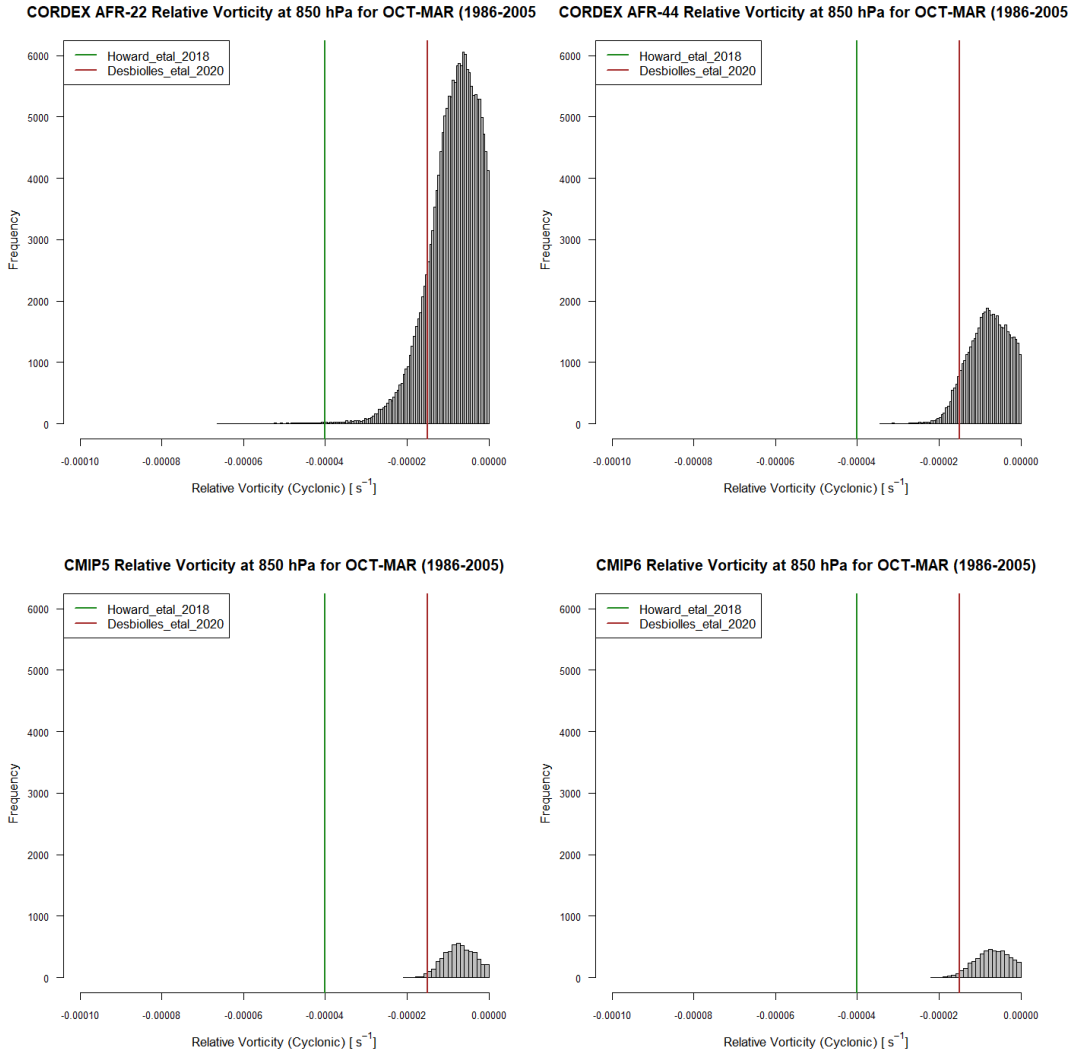

Figure S7: Histogram of relative vorticity for months Oct-Mar during 1986-2005 at 850 hPa for CORDEX-Africa at 0.22º (upper left), for CORDEX-Africa 0.44º (upper right), for CMIP5 (lower left), and for CMIP6 (lower right). Pixels used are enclosed by the region from 14 ºE to 25 ºE and from 11 ºS to 19 ºS. For all histograms mean monthly u and v values are used.

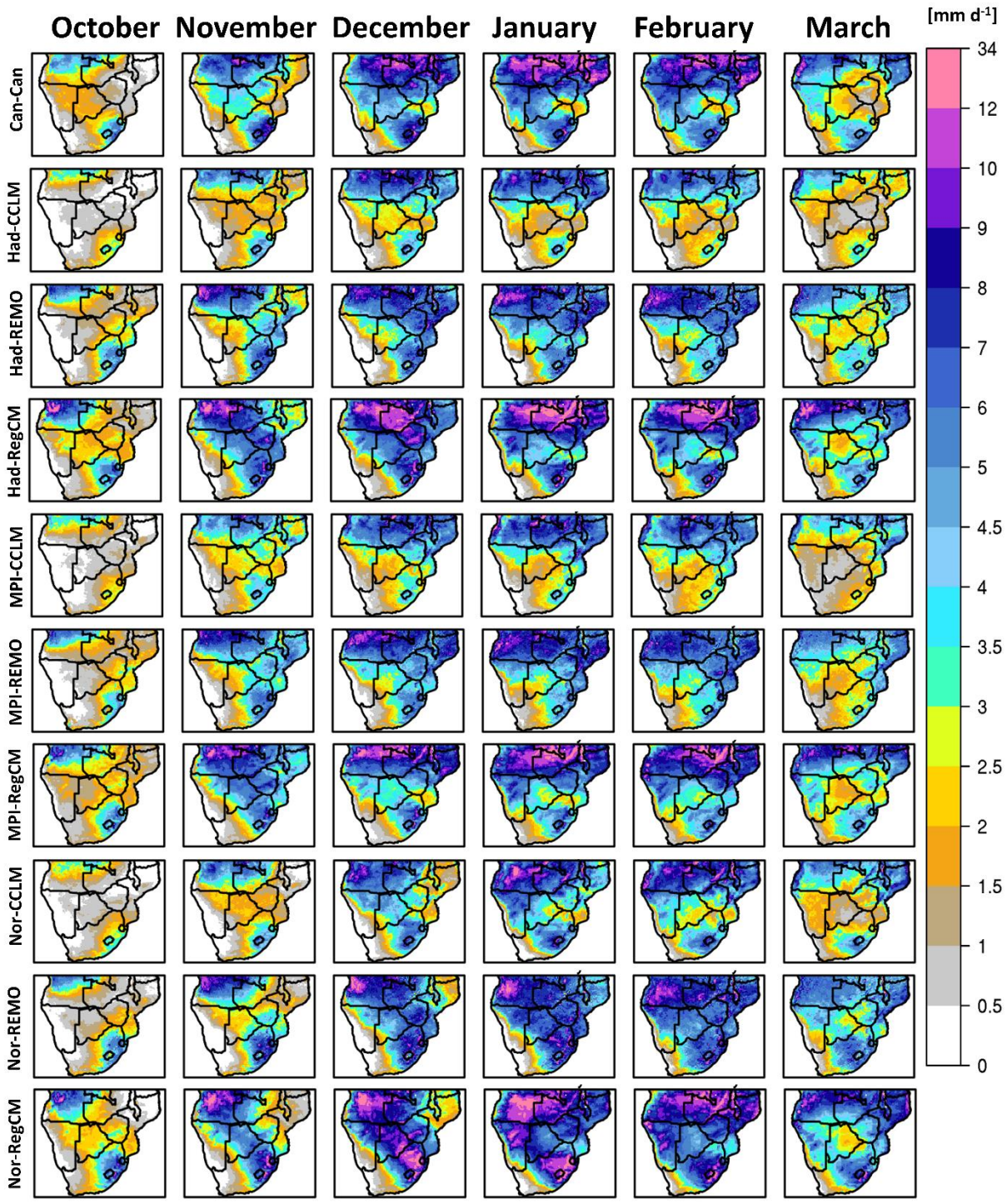

71

72 Figure S8: Monthly precipitation climatologies during the period 1986-2005 in mm d^{-1} from the ensemble members
73 of the CORDEX-Africa 0.22º simulations (CORDEX0.22).

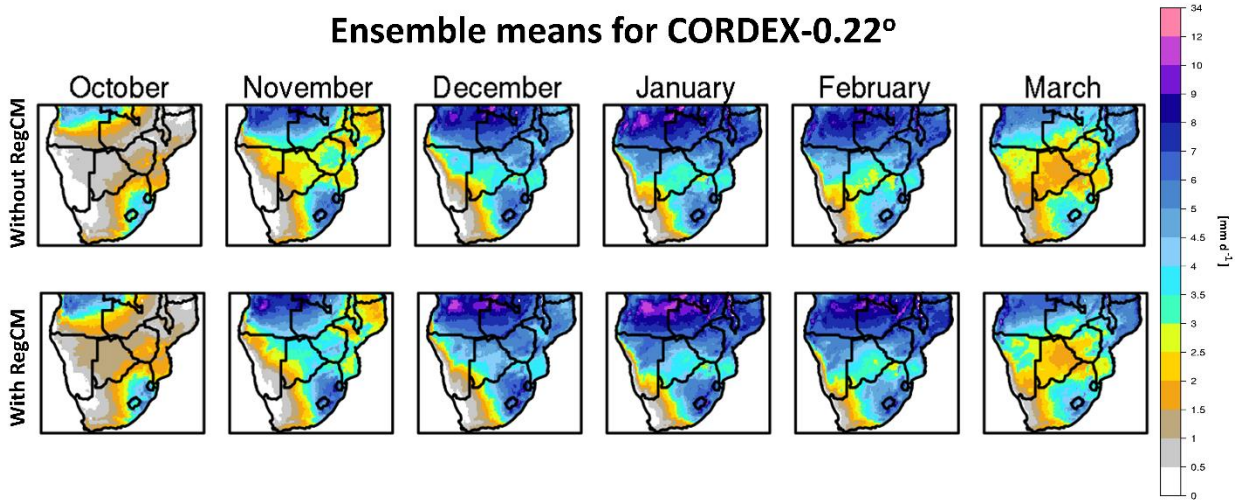

Figure S9: Ensemble mean of the CORDEX-Africa 0.22º ensemble (CORDEX0.22) by excluding the RegCM4-7 simulations (upper row) and by including all available simulations (bottom row).

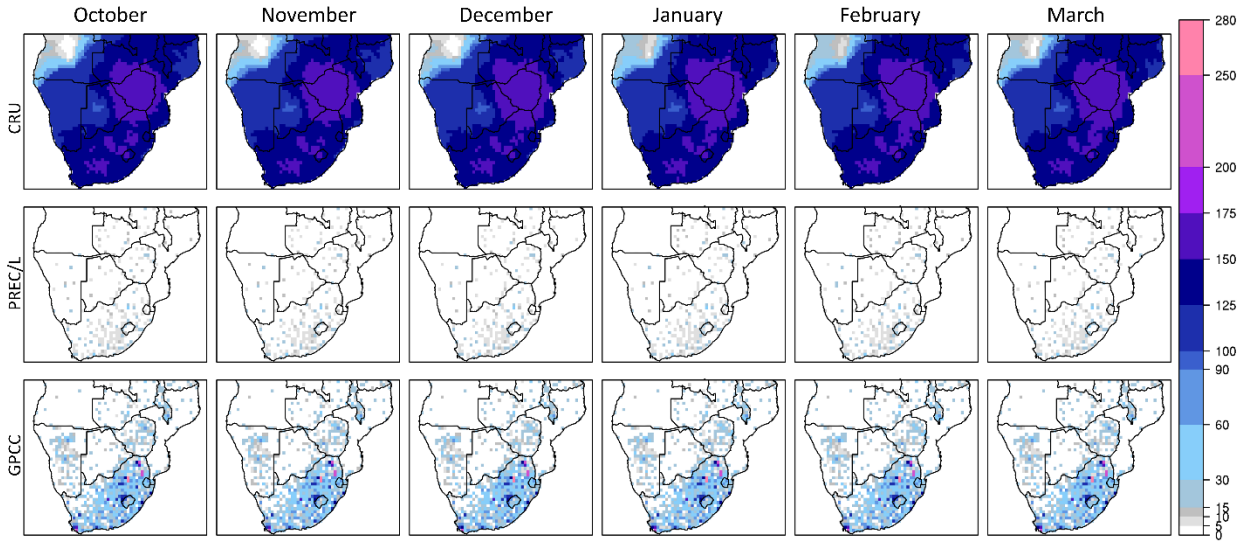

Figure S10. Total number of reporting stations/rain-gauges for each month during the period 1986-2005, used in the interpolation process of each gauge-based product (CRU, PREC/L, GPCC).

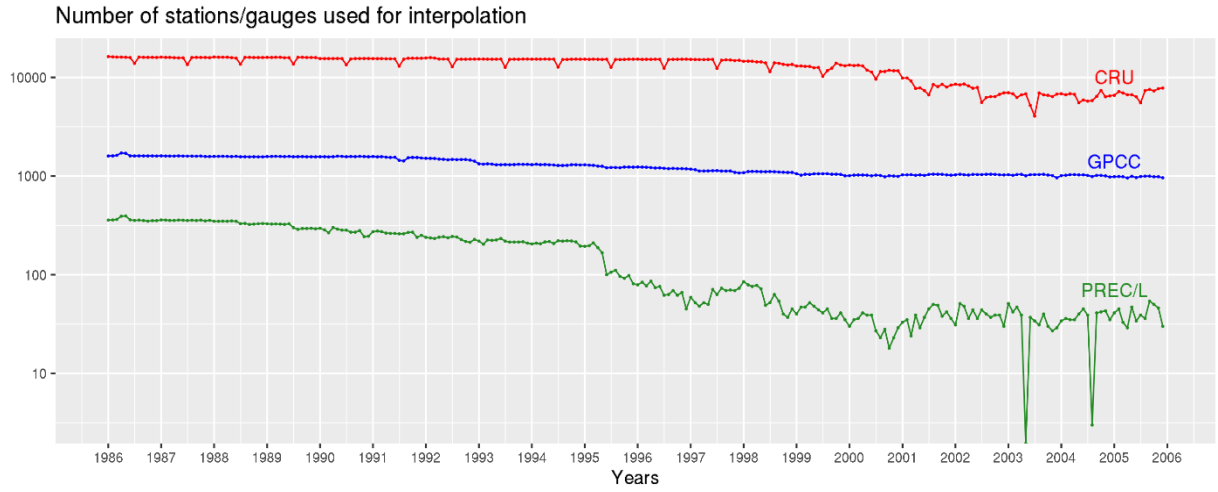

Figure S11. Timeseries of the number of stations/rain-gauges used in 3 gauge-based products, over the southern Africa region (10 ºE to 42 ºE and 10 ºS to 35 ºS).

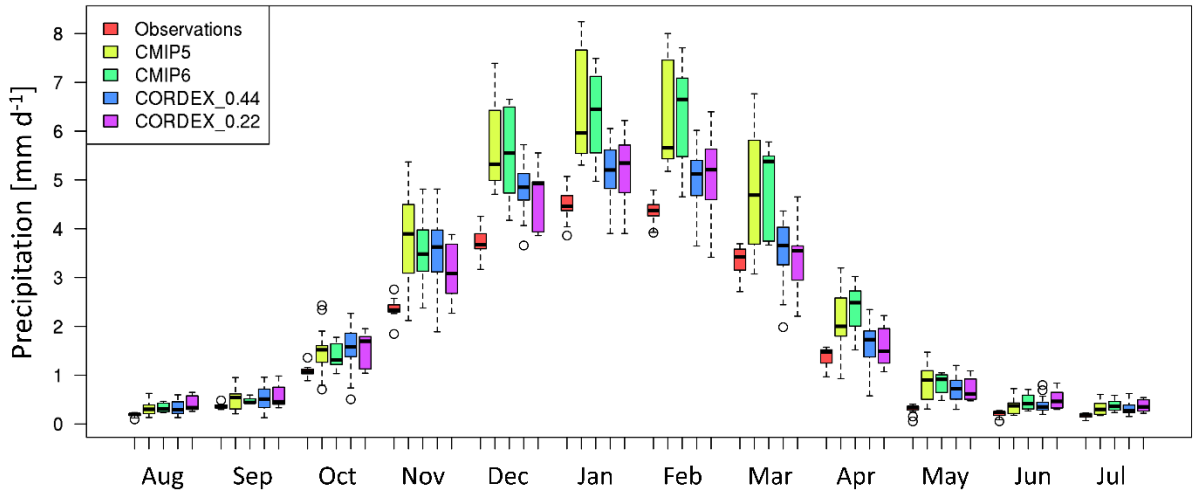

Figure S12: Annual cycle of monthly precipitation during 1986-2005 for the ensemble of observational data (gauge-based, satellite and reanalysis), CMIP5 (Coupled Model Intercomparison Project Phase 5), CMIP6 (Coupled Model Intercomparison Project Phase 6), CORDEX0.44 (Coordinated Regional Climate Downscaling Experiment – Africa domain with a spatial resolution equal to 0.44º x 0.44º) and CORDEX-0.22º (CORDEX-Africa simulations with a spatial resolution equal to 0.22º x 0.22º, excluding the RegCM4-7 simulations from the ensemble). The thick horizontal black lines indicate the ensemble median for each month, the box encloses the interquartile range, and the tails denote the full ensemble range. Circles represent the outliers for each ensemble. Grid points only are considered.

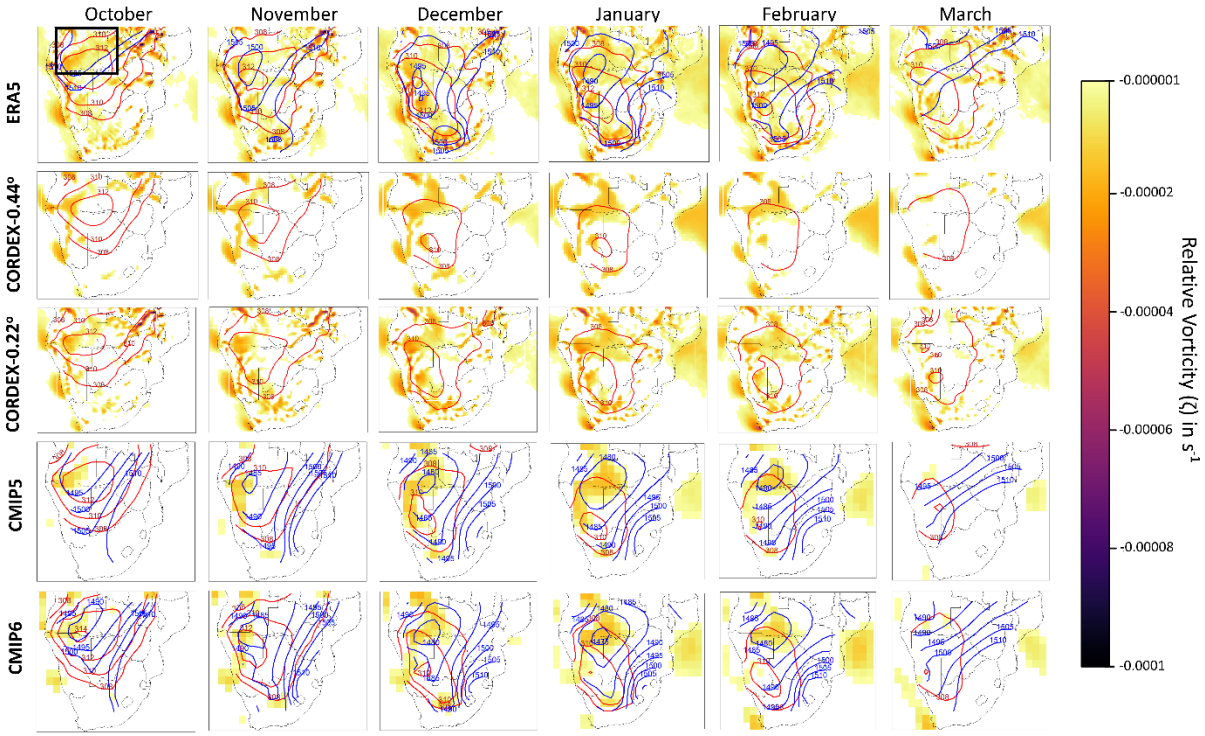

Figure S13: Monthly climatologies of the Angola Low pressure system during the rainy season for the period 1986-2005. Filled contours indicate cyclonic relative vorticity (ζ) for $\zeta < -0.00001$ s^{-1} over the whole southern Africa region. Red lines indicate the isotherms of potential temperature at 850 hPa, having an increment of 2 K. Blue lines indicate isoheights of the geopotential height at 850 hPa, having an increment of 5 m. CORDEX0.44/0.22 are not plotted with geopotential isoheights, because this variable was not available for CORDEX simulations. From top to bottom: ERA5, ensemble mean of CORDEX0.44°, CORDEX0.22°, CMIP5 and CMIP6 simulations. Black box indicates the region from 14 °E to 25 °E and from 11 °S to 19 °S.

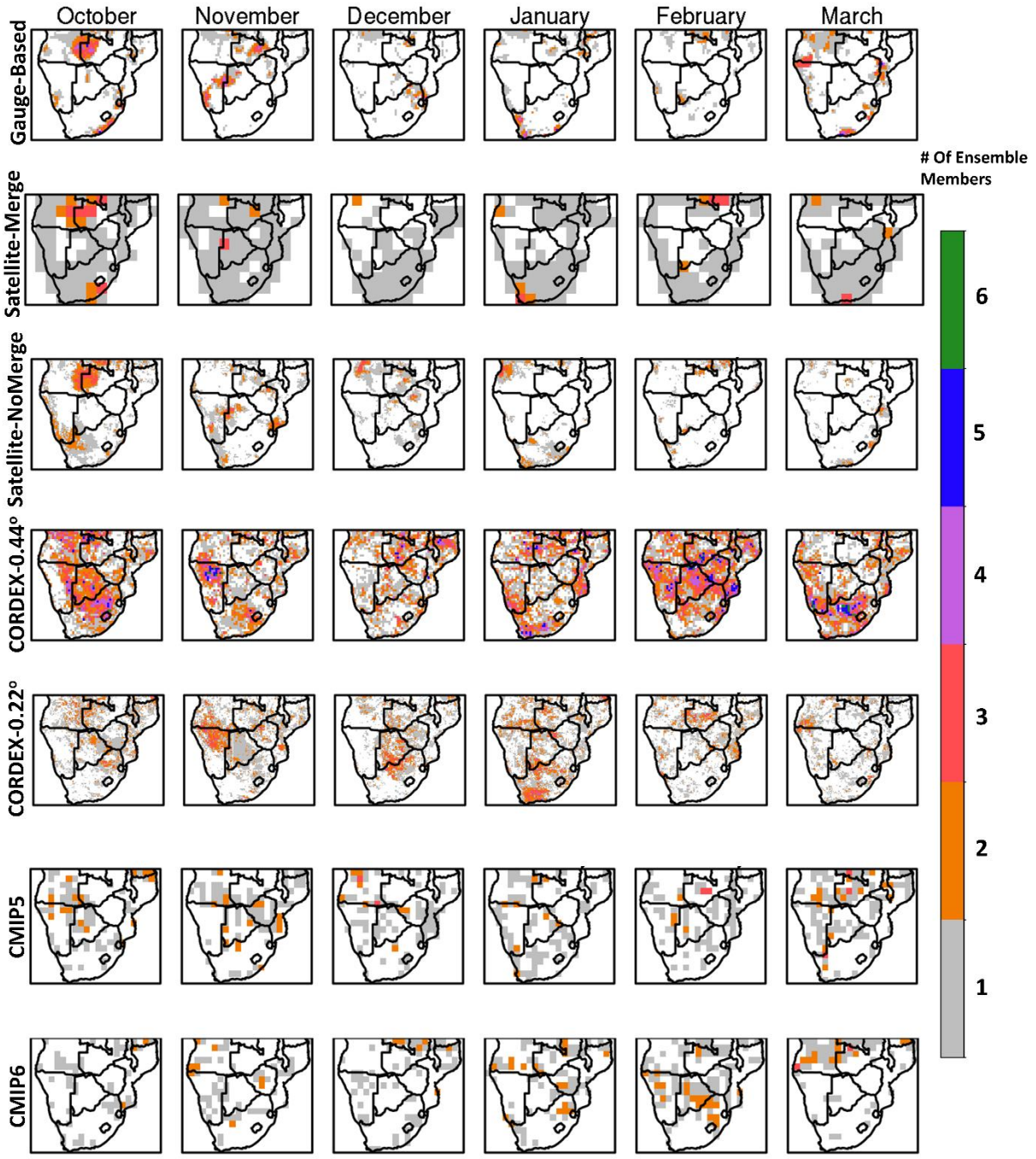

Figure S14. Number of ensemble members yielding statistically significant results for monthly precipitation trends based on the Mann-Kendall test (a=0.05).

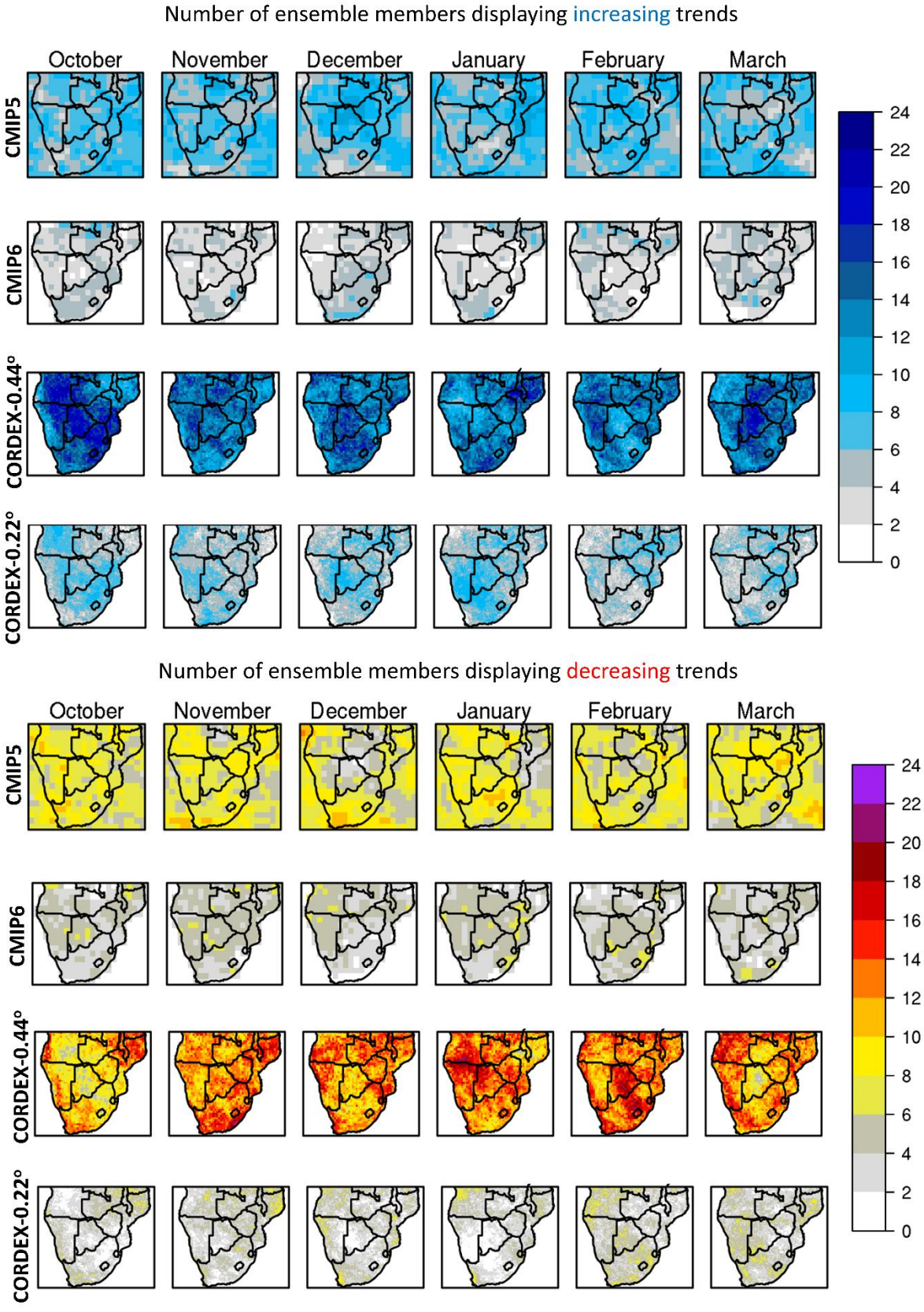
Number of ensemble members displaying increasing trends
October
November
December
January
February
March
CMIP5
CMIP6
CORDEX-0.44°
CORDEX-0.22°
24
22
20
18
16
14
12
10
8
6
4
2
0
Number of ensemble members displaying decreasing trends
October
November
December
January
February
March
CMIP5
CMIP6
CORDEX-0.44°
CORDEX-0.22°
24
22
20
18
16
14
12
10
8
6
4
2
0

Figure S15: Number of ensemble members displaying increasing or decreasing trends for each ensemble.

References

Adler, R.F., Gu, G., Huffman, G.J., 2012. Estimating Climatological Bias Errors for the Global Precipitation Climatology Project (GPCP). J. Appl. Meteorol. Climatol. 51, 84–99. https://doi.org/10.1175/JAMC-D-11-052.1

Ashouri, H., Hsu, K.-L., Sorooshian, S., Braithwaite, D.K., Knapp, K.R., Cecil, L.D., Nelson, B.R., Prat, O.P., 2015. PERSIANN-CDR: Daily Precipitation Climate Data Record from Multisatellite Observations for Hydrological and Climate Studies. Bull. Am. Meteorol. Soc. 96, 69–83. https://doi.org/10.1175/BAMS-D-13-00068.1

Bentsen, M., Bethke, I., Debernard, J.B., Iversen, T., Kirkevåg, A., Seland, Ø., Drange, H., Roelandt, C., Seierstad, I.A., Hoose, C., Kristjánsson, J.E., 2013. The Norwegian Earth System Model, NorESM1-M – Part 1: Description and basic evaluation of the physical climate. Geosci. Model Dev. 6, 687–720. https://doi.org/10.5194/gmd-6-687-2013

C3S, 2017. ERA5: Fifth generation of ECMWF atmospheric reanalyses of the global climate.

CCCma, 2017. Environment and Climate Change Canada - Climate Change - CanESM2 [WWW Document]. URL http://www.ec.gc.ca/ccmac-cccma/default.asp?lang=En&xml=1A3B7DF1-99BB-4EC8-B129-09F83E72D645 (accessed 6.23.20).

Chen, M., Shi, W., Xie, P., Silva, V.B.S., Kousky, V.E., Higgins, R.W., Janowiak, J.E., 2008. Assessing objective techniques for gauge-based analyses of global daily precipitation. J. Geophys. Res. Atmospheres 113. https://doi.org/10.1029/2007JD009132

Chen, M., Xie, P., Janowiak, J.E., Arkin, P.A., 2002. Global Land Precipitation: A 50-yr Monthly Analysis Based on Gauge Observations. J. Hydrometeorol. 3, 249–266. https://doi.org/10.1175/1525-7541(2002)003<0249:GLPAYM>2.0.CO;2

Collins, W.J., Bellouin, N., Doutriaux-Boucher, M., Gedney, N., Halloran, P., Hinton, T., Hughes, J., Jones, C.D., Joshi, M., Liddicoat, S., Martin, G., O'Connor, F., Rae, J., Senior, C., Sitch, S., Totterdell, I., Wiltshire, A., Woodward, S., 2011. Development and evaluation of an Earth-System model – HadGEM2. Geosci. Model Dev. 4, 1051–1075. https://doi.org/10.5194/gmd-4-1051-2011

COSMO, 2020. COSMO core documentation [WWW Document]. URL http://www.cosmo-model.org/content/model/documentation/core/default.htm#p1 (accessed 6.22.20).

Dufresne, J.-L., Foujols, M.-A., Denvil, S., Caubel, A., Marti, O., Aumont, O., Balkanski, Y., Bekki, S., Bellenger, H., Benshila, R., Bony, S., Bopp, L., Braconnot, P., Brockmann, P., Cadule, P., Cheruy, F., Codron, F., Cozic, A., Cugnet, D., de Noblet, N., Duvel, J.-P., Ethé, C., Fairhead, L., Fichefet, T., Flavoni, S., Friedlingstein, P., Grandpeix, J.-Y., Guez, L., Guilyardi, E., Hauglustaine, D., Hourdin, F., Idelkadi, A., Ghattas, J., Joussaume, S., Kageyama, M., Krinner, G., Labetoulle, S., Lahellec, A., Lefebvre, M.-P., Lefevre, F., Levy, C., Li, Z.X., Lloyd, J., Lott, F., Madec, G., Mancip, M., Marchand, M., Masson, S., Meurdesoif, Y., Mignot, J., Musat, I., Parouty, S., Polcher, J., Rio, C., Schulz, M., Swingedouw, D., Szopa, S., Talandier, C., Terray, P., Viovy, N., Vuichard, N., 2013. Climate change projections using the IPSL-CM5 Earth System Model: from CMIP3 to CMIP5. Clim. Dyn. 40, 2123–2165. https://doi.org/10.1007/s00382-012-1636-1

Dunne, J.P., John, J.G., Adcroft, A.J., Griffies, S.M., Hallberg, R.W., Shevliakova, E., Stouffer, R.J., Cooke, W., Dunne, K.A., Harrison, M.J., Krasting, J.P., Malyshev, S.L., Milly, P.C.D., Phillipps, P.J., Sentman, L.T., Samuels, B.L., Spelman, M.J., Winton, M., Wittenberg, A.T., Zadeh, N., 2012. GFDL's ESM2 Global Coupled Climate–Carbon Earth System Models. Part I: Physical Formulation and Baseline Simulation Characteristics. J. Clim. 25, 6646–6665. https://doi.org/10.1175/JCLI-D-11-00560.1

Funk, C., Peterson, P., Landsfeld, M., Pedreros, D., Verdin, J., Shukla, S., Husak, G., Rowland, J., Harrison, L., Hoell, A., Michaelsen, J., 2015. The climate hazards infrared precipitation with stations—a new environmental record for monitoring extremes. Sci. Data 2, 150066. https://doi.org/10.1038/sdata.2015.66

Giorgetta, M.A., Jungclaus, J., Reick, C.H., Legutke, S., Bader, J., Böttinger, M., Brovkin, V., Crueger, T., Esch, M., Fieg, K., Glushak, K., Gayler, V., Haak, H., Hollweg, H.-D., Ilyina, T., Kinne, S., Kornblueh, L., Matei, D., Mauritsen, T., Mikolajewicz, U., Mueller, W., Notz, D., Pithan, F., Raddatz, T., Rast, S., Redler, R., Roeckner, E., Schmidt, H., Schnur, R., Segschneider, J., Six, K.D., Stockhause, M., Timmreck, C., Wegner, J., Widmann, H., Wieners, K.-H., Claussen, M., Marotzke, J., Stevens, B., 2013. Climate and carbon cycle changes from 1850 to 2100 in MPI-ESM simulations for the Coupled Model Intercomparison Project phase 5. J. Adv. Model. Earth Syst. 5, 572–597. https://doi.org/10.1002/jame.20038

Harris, I., Jones, P.D., Osborn, T.J., Lister, D.H., 2014. Updated high-resolution grids of monthly climatic observations – the CRU TS3.10 Dataset. Int. J. Climatol. 34, 623–642. https://doi.org/10.1002/joc.3711

Hazeleger, W., Severijns, C., Semmler, T., Ştefănescu, S., Yang, S., Wang, X., Wyser, K., Dutra, E., Baldasano, J.M., Bintanja, R., Bougeault, P., Caballero, R., Ekman, A.M.L., Christensen, J.H., van den Hurk, B., Jimenez, P., Jones, C., Kållberg, P., Koenigk, T., McGrath, R., Miranda, P., van Noije, T., Palmer, T., Parodi, J.A., Schmith, T., Selten, F., Storelvmo, T., Sterl, A., Tapamo, H., Vancoppenolle, M., Viterbo, P., Willén, U., 2010. EC-EarthA Seamless Earth-System Prediction Approach in Action. Bull. Am. Meteorol. Soc. 91, 1357–1364. https://doi.org/10.1175/2010BAMS2877.1

Held, I.M., Guo, H., Adcroft, A., Dunne, J.P., Horowitz, L.W., Krasting, J., Shevliakova, E., Winton, M., Zhao, M., Bushuk, M., Wittenberg, A.T., Wyman, B., Xiang, B., Zhang, R., Anderson, W., Balaji, V., Donner, L., Dunne, K., Durachta, J., Gauthier, P.P.G., Ginoux, P., Golaz, J.-C., Griffies, S.M., Hallberg, R., Harris, L., Harrison, M., Hurlin, W., John, J., Lin, P., Lin, S.-J., Malyshev, S., Menzel, R., Milly, P.C.D., Ming, Y., Naik, V., Paynter, D., Paulot, F., Rammaswamy, V., Reichl, B., Robinson, T., Rosati, A., Seman, C., Silvers, L.G., Underwood, S., Zadeh, N., 2019. Structure and Performance of GFDL's CM4.0 Climate Model. J. Adv. Model. Earth Syst. 11, 3691–3727. https://doi.org/10.1029/2019MS001829

Hersbach, H., Bell, B., Berrisford, P., Hirahara, S., Horányi, A., Muñoz-Sabater, J., Nicolas, J., Peubey, C., Radu, R., Schepers, D., Simmons, A., Soci, C., Abdalla, S., Abellan, X., Balsamo, G., Bechtold, P., Biavati, G., Bidlot, J., Bonavita, M., Chiara, G.D., Dahlgren, P., Dee, D., Diamantakis, M., Dragani, R., Flemming, J., Forbes, R., Fuentes, M., Geer, A., Haimberger, L., Healy, S., Hogan, R.J., Hólm, E., Janisková, M., Keeley, S., Laloyaux, P., Lopez, P., Lupu, C., Radnoti, G., Rosnay, P. de, Rozum, I., Vamborg, F., Villaume, S., Thépaut, J.-N., 2020. The ERA5 global reanalysis. Q. J. R. Meteorol. Soc. 146, 1999–2049. https://doi.org/10.1002/qj.3803

Jacob, D., Elizalde, A., Haensler, A., Hagemann, S., Kumar, P., Podzun, R., Rechid, D., Remedio, A.R., Saeed, F., Sieck, K., Teichmann, C., Wilhelm, C., 2012. Assessing the Transferability of the Regional Climate Model REMO to Different COordinated Regional Climate Downscaling EXperiment (CORDEX) Regions. Atmosphere 3, 181–199. https://doi.org/10.3390/atmos3010181

Jeffrey, S., Rotstayn, L.D., Collier, M., Dravitzki, S.M., Hamalainen, C., Moeseneder, C., Wong, K., Syktus, J., 2013. Australia ' s CMIP 5 submission using the CSIRO-Mk 3 . 6 model.

Maidment, R.I., Grimes, D., Black, E., Tarnavsky, E., Young, M., Greatrex, H., Allan, R.P., Stein, T., Nkonde, E., Senkunda, S., Alcántara, E.M.U., 2017. A new, long-term daily satellite-based rainfall dataset for operational monitoring in Africa. Sci. Data 4, 170063. https://doi.org/10.1038/sdata.2017.63

Massonnet, F., Ménégoz, M., Acosta, M., Yepes-Arbós, X., Exarchou, E., Doblas-Reyes, F.J., 2020. Replicability of the EC-Earth3 Earth system model under a change in computing environment. Geosci. Model Dev. 13, 1165–1178. https://doi.org/10.5194/gmd-13-1165-2020

Mauritsen, T., Bader, J., Becker, T., Behrens, J., Bittner, M., Brokopf, R., Brovkin, V., Claussen, M., Crueger, T., Esch, M., Fast, I., Fiedler, S., Fläschner, D., Gayler, V., Giorgetta, M., Goll, D.S., Haak, H., Hagemann, S., Hedemann, C., Hohenegger, C., Ilyina, T., Jahns, T., Jimenéz-de-la-Cuesta, D., Jungclaus, J., Kleinen, T., Kloster, S., Kracher, D., Kinne, S., Kleberg, D., Lasslop, G., Kornblueh, L., Marotzke, J., Matei, D., Meraner, K., Mikolajewicz, U., Modali, K., Möbis, B., Müller, W.A., Nabel, J.E.M.S., Nam, C.C.W., Notz, D., Nyawira, S.-S., Paulsen, H., Peters, K., Pincus, R., Pohlmann, H., Pongratz, J., Popp, M., Raddatz, T.J., Rast, S., Redler, R., Reick, C.H., Rohrschneider, T., Schemann, V., Schmidt, H., Schnur, R., Schulzweida, U., Six, K.D., Stein, L., Stemmler, I., Stevens, B., Storch, J.-S. von, Tian, F., Voigt, A., Vrese, P., Wieners, K.-H., Wilkenskjeld, S., Winkler, A., Roeckner, E., 2019. Developments in the MPI-M Earth System Model version 1.2 (MPI-ESM1.2) and Its Response to Increasing CO2. J. Adv. Model. Earth Syst. 11, 998–1038. https://doi.org/10.1029/2018MS001400

Novella, N.S., Thiaw, W.M., 2013. African Rainfall Climatology Version 2 for Famine Early Warning Systems. J. Appl. Meteorol. Climatol. 52, 588–606. https://doi.org/10.1175/JAMC-D-11-0238.1

Samuelsson, P., Gollvik, S., Jansson, C., Kupiainen, M., Kourzeneva, E., van de Berg, W.J., 2015. The surface processes of the Rossby Centre regional atmospheric climate model (RCA4). [WWW Document]. https://www.smhi.se/polopoly_fs/1.89803!/Menu/general/extGroup/attachmentColHold/mainCol1/file/meteorologi_157.pdf. URL https://www.smhi.se/polopoly_fs/1.89803!/Menu/general/extGroup/attachmentColHold/mainCol1/file/meteorologi_157.pdf (accessed 12.9.19).

Schneider, U., Becker, A., Finger, P., Meyer-Christoffer, A., Rudolf, B., Ziese, M., 2015. GPCC Full Data Reanalysis Version 7.0 at 0.5°: Monthly Land-Surface Precipitation from Rain-Gauges built on GTS-based and Historic Data.

Scinocca, J.F., Kharin, V.V., Jiao, Y., Qian, M.W., Lazare, M., Solheim, L., Flato, G.M., Biner, S., Desgagne, M., Dugas, B., 2016. Coordinated Global and Regional Climate Modeling. J. Clim. 29, 17–35. https://doi.org/10.1175/JCLI-D-15-0161.1

Scinocca, J.F., Kharin, V.V., Jiao, Y., Qian, M.W., Lazare, M., Solheim, L., Flato, G.M., Biner, S., Desgagne, M., Dugas, B., 2015. Coordinated Global and Regional Climate Modeling. J. Clim. 29, 17–35. https://doi.org/10.1175/JCLI-D-15-0161.1

Seland, Ø., Bentsen, M., Olivié, D., Toniazzo, T., Gjermundsen, A., Graff, L.S., Debernard, J.B., Gupta, A.K., He, Y.-C., Kirkevåg, A., Schwinger, J., Tjiputra, J., Aas, K.S., Bethke, I., Fan, Y., Griesfeller, J., Grini, A., Guo, C., Ilicak, M., Karset, I.H.H., Landgren, O., Liakka, J., Moseid, K.O., Nummelin, A., Spensberger, C., Tang, H., Zhang, Z., Heinze, C., Iversen, T., Schulz, M., 2020. Overview of the Norwegian Earth System Model (NorESM2) and key climate response of CMIP6 DECK, historical, and scenario simulations. Geosci. Model Dev. 13, 6165–6200. https://doi.org/10.5194/gmd-13-6165-2020

Swart, N.C., Cole, J.N.S., Kharin, V.V., Lazare, M., Scinocca, J.F., Gillett, N.P., Anstey, J., Arora, V., Christian, J.R., Hanna, S., Jiao, Y., Lee, W.G., Majaess, F., Saenko, O.A., Seiler, C., Seinen, C., Shao, A., Sigmond, M., Solheim, L., von Salzen, K., Yang, D., Winter, B., 2019. The Canadian Earth System Model version 5 (CanESM5.0.3). Geosci. Model Dev. 12, 4823–4873. https://doi.org/10.5194/gmd-12-4823-2019

Tarnavsky, E., Grimes, D., Maidment, R., Black, E., Allan, R.P., Stringer, M., Chadwick, R., Kayitakire, F., 2014. Extension of the TAMSAT Satellite-Based Rainfall Monitoring over Africa and from 1983 to Present. J. Appl. Meteorol. Climatol. 53, 2805–2822. https://doi.org/10.1175/JAMC-D-14-0016.1

Tatebe, H., Ogura, T., Nitta, T., Komuro, Y., Ogochi, K., Takemura, T., Sudo, K., Sekiguchi, M., Abe, M., Saito, F., Chikira, M., Watanabe, S., Mori, M., Hirota, N., Kawatani, Y., Mochizuki, T., Yoshimura, K., Takata, K., O'ishi, R., Yamazaki, D., Suzuki, T., Kurogi, M., Kataoka, T., Watanabe, M., Kimoto, M., 2019. Description and basic evaluation of simulated mean state, internal variability, and climate sensitivity in MIROC6. Geosci. Model Dev. 12, 2727–2765. https://doi.org/10.5194/gmd-12-2727-2019

van Meijgaard, E., van Ulft, L.H., van de Berg, W.J., Bosveld, F.C., van den Hurk, B.J.J.M., Lenderink, G., Siebesma, A.P., 2008. The KNMI regional atmospheric climate model RACMO version 2.1 (TR - 302). KNMI, The Netherland.

Voldoire, A., Saint-Martin, D., Sénési, S., Decharme, B., Alias, A., Chevallier, M., Colin, J., Guérémy, J.-F., Michou, M., Moine, M.-P., Nabat, P., Roehrig, R., Mélia, D.S. y, Séférian, R., Valcke, S., Beau, I., Belamari, S., Berthet, S., Cassou, C., Cattiaux, J., Deshayes, J., Douville, H., Ethé, C., Franchistéguy, L., Geoffroy, O., Lévy, C., Madec, G., Meurdesoif, Y., Msadek, R., Ribes, A., Sanchez-Gomez, E., Terray, L., Waldman, R., 2019. Evaluation of CMIP6 DECK Experiments With CNRM-CM6-1. J. Adv. Model. Earth Syst. 11, 2177–2213. https://doi.org/10.1029/2019MS001683

Voldoire, A., Sanchez-Gomez, E., Salas y Mélia, D., Decharme, B., Cassou, C., Sénési, S., Valcke, S., Beau, I., Alias, A., Chevallier, M., Déqué, M., Deshayes, J., Douville, H., Fernandez, E., Madec, G., Maisonnave, E., Moine, M.-P., Planton, S., Saint-Martin, D., Szopa, S., Tyteca, S., Alkama, R., Belamari, S., Braun, A., Coquart, L., Chauvin, F., 2013. The CNRM-CM5.1 global climate model: description and basic evaluation. Clim. Dyn. 40, 2091–2121. https://doi.org/10.1007/s00382-011-1259-y

Watanabe, M., Suzuki, T., O'ishi, R., Komuro, Y., Watanabe, S., Emori, S., Takemura, T., Chikira, M., Ogura, T., Sekiguchi, M., Takata, K., Yamazaki, D., Yokohata, T., Nozawa, T., Hasumi, H., Tatebe, H., Kimoto, M., 2010. Improved Climate Simulation by MIROC5: Mean States, Variability, and Climate Sensitivity. J. Clim. 23, 6312–6335. https://doi.org/10.1175/2010JCLI3679.1

Willmott, C.J., Matsuura, K., 1995. Smart Interpolation of Annually Averaged Air Temperature in the United States. J. Appl. Meteorol. 34, 2577–2586. https://doi.org/10.1175/1520-0450(1995)034<2577:SIOAAA>2.0.CO;2

Xie, P., Arkin, P.A., 1997. Global Precipitation: A 17-Year Monthly Analysis Based on Gauge Observations, Satellite Estimates, and Numerical Model Outputs. Bull. Am. Meteorol. Soc. 78, 2539–2558. https://doi.org/10.1175/1520-0477(1997)078<2539:GPAYMA>2.0.CO;2